Supporting Information

Exceptional visible-light-driven photocatalytic activity over BiOBr–$ZnFe_2O_4$ heterojunctions

Liang Kong,[a] Zheng Jiang,*[a,b] Tiancun Xiao,[a] Lufeng Lu,[a] Martin O. Jones[a, c] and Peter P. Edwards*[a]

[a] *Department of Chemistry, Inorganic Chemistry Laboratory, University of Oxford, Oxford, OX1 3QR, UK; Tel: 44(0)1865 272646 Email: peter.edwards@chem.ox.ac.uk*
[b] *Jesus College, University of Oxford, Oxford, OX1 3DW, U.K; Tel: 44(0)1865 272660 Email: zheng.jiang@chem.ox.ac.uk*
[c] *Rutherford Appleton Laboratory, Harwell Science and Innovation Campus, Didcot, UK*

1. Synthesis of $ZnFe_2O_4$ precursor

All the reagents and solvents for synthesis and analysis are commercially available and used without further treatment. $ZnFe_2O_4$ was synthesised by co-precipitation method. In brief, stoichiometric amounts of $Zn(CH_3COO)_2$ (AR, BDH, 96.0%) and $Fe(NO_3)_3{\cdot}9H_2O$ (AR, Aldrich, 97.0%) were dissolved in 200 mL distilled water under magnetic stirred for 20 minutes. Then 2M $NaOH/Na_2CO_3$ was dropped into the solution to adjust the pH to a range of 9-10. After rigorously stirring for another 30 minutes, the precursor suspension was aged overnight. The resulting precipitate was filtered, washed with distilled water, and then dried at 65°C overnight. The as-synthesised product was calcined at 800 °C for 6 hours to form the spinel structure.

2. Preparation of BiOBr-$ZnFe_2O_4$ samples

In a typical synthesis, a measured amount of $Bi(NO_3)_3{\cdot}5H_2O$ (AR, Sigma Aldrich, 99.0%) and $ZnFe_2O_4$ were dissolved in 100mL aqueous solution containing 5mL acetic acid (HAc). The solution was mixed with varied amount of $Bi(NO_3)_3{\cdot}5H_2O$ in order to obtain BiOBr-$ZnFe_2O_4$ with molar ratio of 1:9, 5:5, 9:1, respectively. The mixture was vigorously stirred for 30 minutes at room temperature, and the resulting solution was added rapidly to 30mL of de-ionized water containing stoichiometric amounts of KBr (AR, BDH, 99.0%). Upon the adding of mixed solution, light purple precipitates were immediately observed. After stirred for another 30 minutes at room temperature, the suspension was aged for 3 hours; the resulting precipitate was filtered, washed thoroughly with distilled water, and then dried at 65°C overnight.

3. Characterisation

Powder X-ray diffraction (PXRD) measurements of all the prepared samples were performed on a PANanalytical X'Pert PRO diffractometer using monochromatised Cu Kα radiation (source light at the wavelength (λ) of 0.15418nm). The accelerating voltage and applied current were 45KV and 40mA,

respectively. The diffraction angles (2Θ) were scanned over the range between 7°and 80° with a scan rate of $0.03°\cdot s^{-1}$ and step size of 0.008°.

The morphology of the BiOBr-$ZnFe_2O_4$ were characterised using a Field Emission Scanning Electron Microscopy (S-4800 UHR FESEM) with an accelerating voltage of 5.0kV. The doping concentration was verified by EDAX (SERION ESEM). The SEM images of 0.5BiOBr-0.5$ZnFe_2O_4$ and BiOBr; and EDS of 0.9BiOBr-0.1$ZnFe_2O_4$ are presented in Fig. S1.

Light absorption properties were measured using UV-Vis DRS (Cary, UV-5000) with a wavelength range of 200-800nm. The received UV-Vis-DRS results are presented in Fig. S2.

The measurements of magnetic resonance spectra were performed on a conventional X-band (v=9.4GHz) CW ESR spectrometer (Bruker EMX) with 100 kHz magnetic field modulation. The measurements were carried out at room temperature.

4. Photocatalytic degradation of Rhodamine B under visible light

Photocatalytic activities of the BiOBr-$ZnFe_2O_4$ powders were evaluated by the degradation of rhodamine B (RhB) aqueous solution under visible light irradiation. The optical system used for the photocatalytic reaction consisted of an overhead 300W Xenon lamp (PLS-SXE300, Beijing TrustTech) equipped with a UV cutoff filter (UVCUT400, Beijing TrustTech) was used as the visible-light source. In each experiment, 0.1g photocatalyst was dispersed into 100mL of RhB in aqueous solution (20mg/L). Prior to irradiation, the suspensions were syncopated in dark for 1hour to ensure the establishment of absorption-desorption equilibrium of the dye on the surface of catalysts. During the absorption and irradiation process, at time intervals of 10 minutes, approximately 3mL of suspension is collected and then the slurry samples including the photocatalyst and RhB solution were centrifuged (1400rpm, 4 minutes) to remove the photocatalyst particles [1]. The solutions were analyzed by a Perkin-Elmer Lamda 750S UV-visible spectrophotometer, and the characteristic absorption peak of RhB at 553nm is used to determine the extent of RhB degradation.

5. Morphology, EDS, UV-Vis Diffuse Reflectance and Electron Spin Resonance Spectra

The SEM images of 0.5BiOBr-0.5$ZnFe_2O_4$ and BiOBr; and EDS of 0.9BiOBr-0.1$ZnFe_2O_4$ are presented in Fig. S1. It can be seen from Fig. S1 (a) and (b) that the 0.5BiOBr-0.5$ZnFe_2O_4$ and BiOBr have almost the similar flake-like morphology, which are distinct with the spherical morphology of 0.9BiOBr-0.1$ZnFe_2O_4$. The EDS result of the 0.9BiOBr-0.1$ZnFe_2O_4$ in Fig. 1(c) reveals that Pt, Bi, O, Br, Zn and Fe elements coexist in the BiOBr-ZnFe2O4 composite materials, where Pt comes from the spray-coated Pt to eliminate the surface charge in EDAX test.

Fig. S2 shows the UV-Vis-DRS spectra of the BiOBr-$ZnFe_2O_4$ composite photocatalysts, where the absorption edge has been extended considerably in comparison with the pure BiOBr sample. The bandgap of our samples lies in between 2.87eV and 1.70 eV with a disproportional absorption of light in the visible-light region, suggesting the presence of interactions between $ZnFe_2O_4$ and BiOBr. Moreover, BiOBr-$ZnFe_2O_4$ composite

photocatalysts with such energy bandgaps are very promising for the utilisation of visible-light in comparison with TiO_2 with a wide bandgap of around 3.2eV[2].

ESR spectrum of $ZnFe_2O_4$ (Fig. S3) shows a very intense, single broad signal with a g value of around 2.003, which is attributed to the paramagnetic centres, i.e. Fe^{3+} [3]. As the loading of BiOBr increases, the signals gradually become broader and less intensive.

6. Reaction and Sorption Kinetics

Fig. S4 and S5 demonstrated the photocatalytic activity rate constants and adsorption/desorption equilibrium plots of RhB molecules on the surface of BiOBr-$ZnFe_2O_4$ composite photocatalysts.

The derived k values from Fig. S4 were listed in Table 1 for comparison.

As shown in Fig. S5, the dependence of Rh.B adsorption/desorption equilibrium on contact time between RhB and BiOBr-$ZnFe_2O_4$ series samples suggests that the saturated equilibrium can be reached after 40min. Although the order of adsorption capacity for the BiOBr-$ZnFe_2O_4$ photocatalysts in the sequence as 0.9BiOBr-0.1$ZnFe_2O_4$ > 0.5BiOBr-0.5$ZnFe_2O_4$ > 0.1BiOBr-0.9$ZnFe_2O_4$., their saturated sorption capability is not proportional with the activity order. In addition, the equilibrium results can indirectly reflect the surface area of the samples.

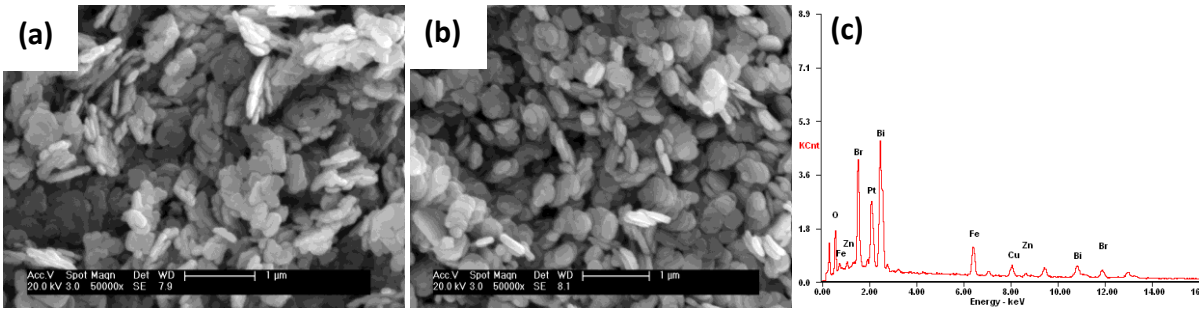

Figure S1 (a, b) SEM images of 0.5BiOBr-0.5$ZnFe_2O_4$ and BiOBr; and (**c**) EDS of 0.9BiOBr-0.1$ZnFe_2O_4$

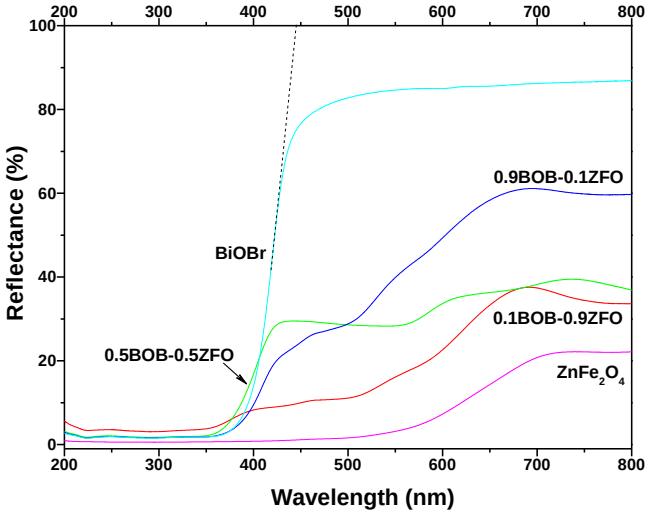

Figure S2 UV-Vis DRS spectra of as-synthesised BiOBr-$ZnFe_2O_4$ samples

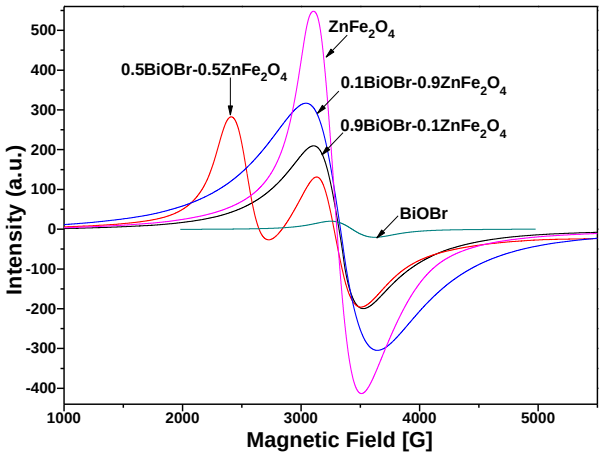

Figure S3 ESR spectra of as-syntheised BiOBr-$ZnFe_2O_4$ samples

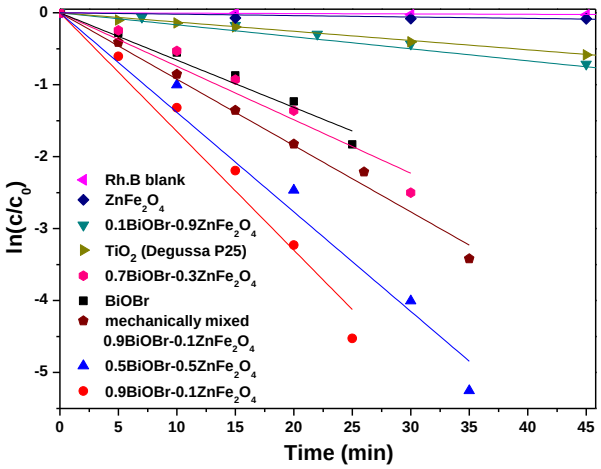

Figure S4 Photocatalytic removal of Rh.B as a function of irradiation time

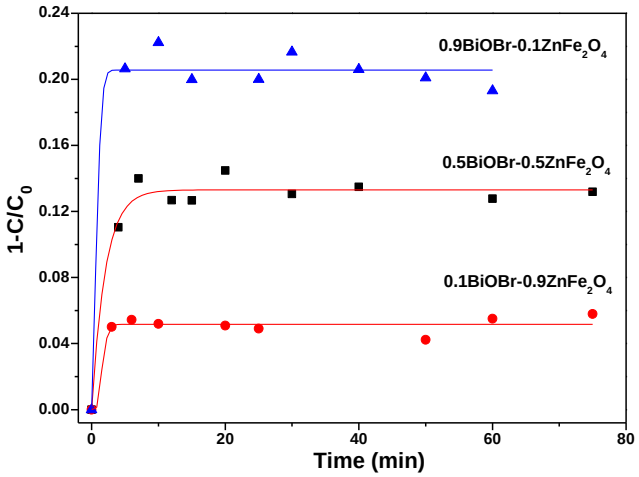

Figure S5 The adsorption equilibrium of BiOBr-$ZnFe_2O_4$ samples

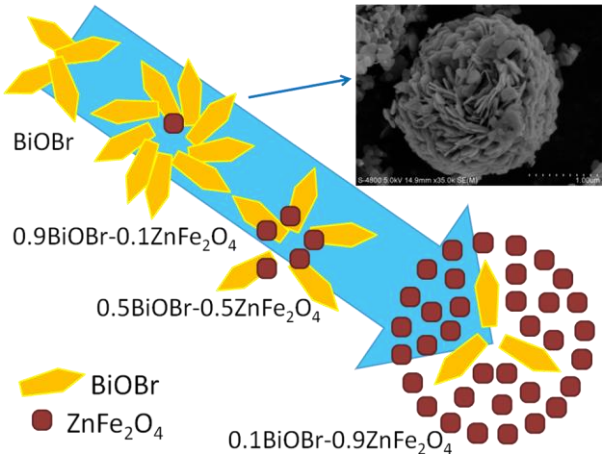

Figure S6 Schematic assembly of the BiOBr-$ZnFe_2O_4$ heterojunctions

1. M. Shang, WenzhongWang and L. Zhang, *Journal of Hazardous Materials* 2009, **167** 803–809.
2. X. Zhang, *The journal of physical chemistry. C*, 2008, **112**, 747-753.
3. X. Li, G. Lu and S. Li, *Journal of Alloys and Compounds*, 1996, **235**, 150-155.